Polymer 49 (2008) 5504–5512

Contents lists available at ScienceDirect

Polymer

journal homepage: www.elsevier.com/locate/polymer

Sequentially adsorbed electrostatic multilayers of polyaniline and azo polyelectrolytes

Haoyu Zhang, Xuejia Yan, Yanwei Wang, Yonghong Deng, Xiaogong Wang*

Department of Chemical Engineering, Laboratory for Advanced Materials, Tsinghua University, Beijing 100084, PR China

ARTICLE INFO

Article history:
Received 3 April 2008
Received in revised form 27 August 2008
Accepted 30 September 2008
Available online 10 October 2008

Keywords:
Polyaniline
Azo-polyelectrolyte
Multilayer

ABSTRACT

In this study, multilayer films composed of alternate polyaniline (PANI) and azo-polyelectrolyte (PNACN, PPAPE, PNANT or PNATZ) layers were fabricated through the electrostatic layer-by-layer self-assembly scheme. In the electrostatic adsorption process, PANI was used as the polycation and the azo polyelectrolytes were used as the polyanion. The multilayer growth was monitored by UV–vis spectroscopy and optical ellipsometry. The photoresponsive and electrochromic properties of the multilayer films were studied by UV–vis spectroscopy and electrochemical measurement. Results show that the multilayer films exhibit linear increases in both the absorbance and film thickness with the increase of the deposition cycles. The thickness contributed by each individual layer depends on the pH of the PANI and azo-polyelectrolyte dipping solutions. The multilayer films can show photoinduced dichroic properties contributed by the azo-polyelectrolyte layers, but the ability to form surface-relief-grating (SRG) upon Ar^+ laser irradiation is relatively weak. The multilayer films possess the characteristic absorption bands related to the azo chromophores and PANI. As the location of the PANI bands depends on its oxidation states, the multilayer films can show sensitive electrochromic variation. For instance, the PANI/PNACN multilayer films can undergo a transition from transparent yellow-green through deep green to opaque black when the potential changes from −0.1 to 0.8 V. It is demonstrated that using the azo polyelectrolytes with different hues, enriched spectrum of the colors can be obtained by the electrochemical transitions. The multilayer films containing both photoresponsive and electroactive components can be expected for applications in optics, photonic devices and others.

1. Introduction

The electrostatic layer-by-layer (LBL) deposition method, introduced by Decher et al., is a versatile way to fabricate a variety of polymeric multilayer films [1–5]. In a typical process, the polyelectrolyte multilayer films are sequentially built-up on proper substrates by alternately dipping in dilute solutions of polycation and polyanion. The total thickness of the polyelectrolyte multilayer films depends on the thickness of each single layer and the number of bilayers. The single layer thickness can be controlled by adjusting the factors such as the concentration, pH and ion strength of the dipping solutions [6–11]. Theoretically, this approach is feasible for almost all types of the polyelectrolytes and other charged particles. A variety of commercial available polyelectrolytes have been applied for the multilayer preparation. The electrostatic LBL self-assembly technique has also been accomplished by using latex particles [12], dendrimers [13], proteins [14], DNA [15] and viruses [16], among others. Construction of self-assembling multilayers to contain functional polyelectrolytes is an important application area of the LBL methodology, which can develop a variety of new functional materials based on the well-defined layered structures and various molecular architectures [5].

Conductive polymers (CPs), which have many interesting optical and electric properties, have aroused tremendous research enthusiasm in past decades [17–22]. Water-soluble/dispersible CPs or precursors have been used for the multilayer build-up since the very early development stage of the electrostatic LBL self-assembly technique [6–8]. Negatively and positively charged conjugated polymers, such as poly(thiophene-3-acetic acid) (PTAA), sulfonated polyaniline (SPANI), and poly(*p*-phenylenevinylene) (PPV) precursor have been used to fabricate electrostatic multilayers together with polyelectrolytes containing counter-ions [6,7]. Polyaniline (PANI) is one of the most important CPs due to its synthetic easiness, low-cost and environmental stability. As it is insoluble in most of the solvents, PANI cannot be directly used for preparing multilayer films through electrostatic deposition. Rubner et al. have developed a route to disperse partially doped PANI in water, which is stable and can be used as a polycation dipping solution in electrostatic LBL self-assembly

* Corresponding author. Tel.: +86 10 62784561; fax: +86 10 62796171.
E-mail address: wxg-dce@mail.tsinghua.edu.cn (X. Wang).

0032-3861/$ – see front matter © 2008 Elsevier Ltd. All rights reserved.
doi:10.1016/j.polymer.2008.09.063

process [8]. By this method, PANI and sulfonated polystyrene (PSS) multilayer films have been prepared and their electrochemical and current–voltage properties have been studied [8,23]. More recently, PANI and PSS have also been used to prepare the core-shell structures on the polystyrene colloidal particles [24]. Electrochromic multilayers have been fabricated by using PANI and negatively ionized nanoparticles of iron-hexacyanoferrate (Prussian Blue), which can show multiple color change upon the oxidation [25].

Azobenzene-containing polymers (azo polymers for short) have been intensively investigated in recent years [26,27]. Azobenzenes are well known for their reversible *trans–cis* isomerization upon light irradiation [28]. Induced by the photoisomerism, azo polymers can show a variety of photoresponsive properties, such as photoinduced birefringence and dichroism [29,30], light-driven command surface [31], optical switching [32], and photoinduced surface-relief-grating (SRG) formation [33,34]. The electrostatic layer-by-layer self-assembly is a feasible way to promise the photonic applications of azo polyelectrolytes. Multilayers containing azo polyelectrolytes have been prepared by sequential electrostatic adsorption, which can show optical second-harmonic generation (SHG) without electric-field poling [35–37]. Electrostatic multilayer films composed of azo polyelectrolytes can also show interesting properties such as photo switching [38], film optical thickness change [39], and surface hydrophilicity variation [39,40]. Ionenes containing rigid azobenzene chromophores separated by flexible spacers have been used to construct internally ordered multilayers through the electrostatic LBL deposition method [41]. The layer-by-layer self-assembly of the ionenes can be adjusted by the *trans–cis* isomerization of the azobenzenes. Use of *cis*-rich ionene solution was found to adsorb up to three times more material at each dipping cycle as compared with the solution of the *trans* counterpart. The polyelectrolytes containing branched azo side-chains have been used to construct photoresponsive multilayers through the sequential electrostatic deposition [42]. The aggregation state of the azo chromophores in the multilayers can be adjusted by selecting the proper dipping solution conditions.

Sequential LBL adsorption method can be extended to introduce both the conductive polymers such as PANI and azo polyelectrolytes in the electrostatic multilayer films. Possible interesting properties of such systems can be partially anticipated from the study on polyaniline (PANI) containing azo functional groups. PANI bearing azo chromophores has been prepared by using horseradish peroxidase catalyzed oxidations [43], and by doping PANI with azobenzenesulfonic acid (ABSA) [44]. The azobenzene-containing PANIs can exhibit *trans–cis* photoisomerization upon the irradiation of UV light. For thin film applications, the sequentially assembled multilayers could be more versatile candidates for structure design and control. The functional polyelectrolytes can be assembled into the multilayer films in the alternate way or other predetermined manners by using suitable counter-polyions. The multilayer thickness can be controlled by adjusting the factors such as the number of dipping cycles, pH and dipping solution composition. Such thin films can combine interesting electroactive and photoresponsive properties related to the functional polymers. However, to our knowledge, a systematic study on the electrostatic multilayers composed of azo polyelectrolytes and polyaniline (or even other water-soluble conductive polymers) is still lacking in the literature.

In this work, the electrostatic layer-by-layer adsorption technique was used to build-up multilayer films of PANI and azobenzene-containing polyelectrolytes. Four types of azo polyelectrolytes, which contain azobenzene or pseudo-stilbene type azo chromophores [45], were used for the exploration. The self-assembly processes were characterized by both UV–vis spectroscopy and optical ellipsometry. The electrochemical and photoresponsive properties of these multilayer films were studied in some detail. The experimental methods, results and discussion will be presented in the following parts.

2. Experimental section

2.1. Materials

Milli-Q water (resistivity > 18 MΩ cm) used in the self-assembly process was obtained from a Millipore water purification system. All other solvents and reagents were purchased commercially as analytical grade products and used directly without further purification. Polyaniline (PANI) was prepared through the oxidative polymerization of aniline in the HCl solution containing a proper amount of ammonium peroxydisulfate and then the product was dunked in ammonia for 24 h to obtain PANI in the Emeraldine form [46]. The azo polyelectrolytes (PPAPE, PNACN, PNANT and PNATZ) were synthesized in authors' laboratory. The chemical structures of the azo polyelectrolytes are given in Fig. 1. The synthesis and characterization of PPAPE have been given in the previous report [40]. The degree of functionization (DF) of PPAPE is 14.9%. The number-averaged molecular weight (M_n) of PPAPE is 48,000 obtained by gel permeation chromatography (GPC). The synthetic processes of PNACN, PNANT and PNATZ are similar to that described in the previous report [42,47]. The azo polyelectrolytes were prepared by the postpolymerization azo-coupling reaction between the precursor polymer bearing the anilino moieties and the diazonium salt of 4-cyanoaniline, 4-nitroaniline, or 2-amino-5-nitrothiazole. As the precursor polymer from the same batch was used for the azo-coupling reaction, these three azo polyelectrolytes had the same DF of 27.7%. The number-averaged molecular weight (M_n) of PNACN, PNANT and PNATZ was estimated to be 16,000, 16,600 and 16,800, respectively. The synthesis and characterization details of PNACN, PNANT and PNATZ are given in Supplementary data.

2.2. Multilayer fabrication

The PANI dipping solutions were prepared by using the procedure reported by Rubner et al. [8]. The Emeraldine-base PANI was dissolved in *N*,*N*-dimethyl-acetamide (DMAc) (10 mg/mL) by first stirring the solution overnight and then sonicating it for another 8–10 h. The PANI aqueous solution was prepared by slowly mixing

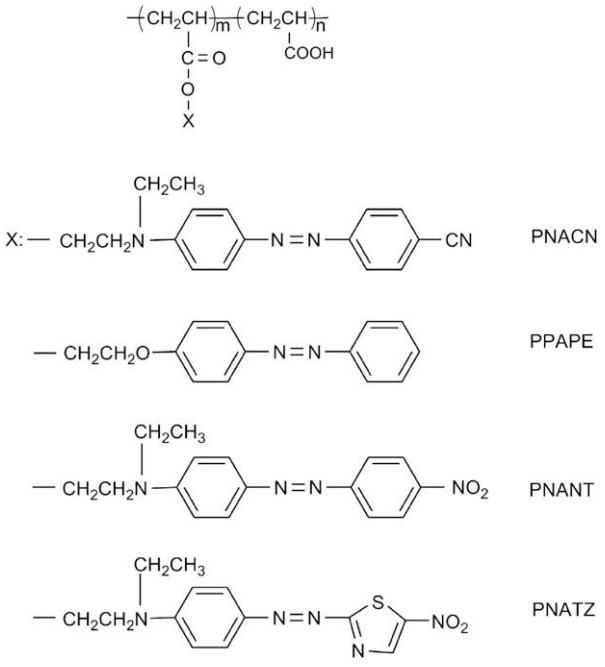

Fig. 1. Chemical structure of the four azo polyelectrolytes.

one part (by volume) of the DMAc solution with nine parts of water, whose pH was adjusted to about 2.5–3.0 with HCl. The dipping solutions were filtered though 0.45 μm membrane before use. The azo polyelectrolytes were dissolved in deionized water by first adjusting the media to alkalinity with NaOH and then neutralizing the solutions with HCl. The concentrations of the dipping solutions were adjusted to 0.25 mg/mL. The quartz, glass and silica slides were pretreated in hot 98% H_2SO_4/30% H_2O_2 (Piranha solution) for 2 h and then in NH_4OH/H_2O_2 (v:v = 3:1) for 3 h, which were thoroughly rinsed with deionized water after each treating step. The multilayer films were prepared by alternately dipping the substrates in the PANI and azo-polyelectrolyte dipping solutions. In the processes, the substrates were immersed in each solution for 10 min and subsequently rinsed with the excess water. After each dipping and rinsing step, the films were blown to dry by clean air stream.

2.3. Characterization

UV–vis spectra of the self-assembled films were recorded on a Perking–Elmer Lambda bio-40 spectrophotometer. Thickness of the multilayer films on silicon wafers was determined by using an optical ellipsometer (SE400, Sentech Instruments) with a He–Ne laser (632.8 nm) at an incident angle of 70° as the light source. The cyclic voltammograms were obtained by using CHI660A Electrochemical Station in a one-compartment three-electrode cell configuration with a platinum sheet (0.5×1 cm^2) as counter electrode and Ag/AgCl as the reference electrode. The electrochromism of the multilayer films was studied by recording the spectral variation with an Agilent 8453 spectrophotometer. In the process, the multilayer films were immersed in water in a quartz cell using Ag wires as the counter electrode and reference electrode. The surface images of the multilayers were monitored using an atomic force microscope (Nanoscope IIIa, tapping mode) and a scanning electron microscope (S-4500, Hitachi).

3. Results and discussion

Four-type azo polyelectrolytes (PPAPE, PNACN, PNANT and PNATZ) were used together with PANI to construct the electrostatic multilayer films. The chemical structures of the azo polyelectrolytes are given in Fig. 1, which are random copolymers composed of the azobenzene-bearing units and acrylic acid units. According to the definition given by Rau [45], the azo chromophores tethered to PPAPE side-chains belong to the azobenzene type, while those of PNACN, PNANT and PNATZ are owned by the pseudo-stilbene type. The two-type azo chromophores can be distinguished by their spectroscopic features and isomerization behavior. The azobenzene-type chromophores usually show strong absorption in UV range. Their *cis*-form is relatively stable and can be easily detected by the UV–vis spectroscopy. The pseudo-stilbene type chromophores have strong absorption in the visible-light range and can undergo rapid *trans–cis–trans* isomerization cycles upon the light irradiation. One of most pertinent properties related to the current study is the different hues of the azo polyelectrolytes, which can supplement the color change caused by the electrochemical variation of PANI.

The azo polyelectrolytes could be well dissolved in aqueous media and used as polyanions for the electrostatic adsorption. PANI used in this study was partially doped, which contained the positive charges on the main-chains in the acidic condition [8]. The dilute aqueous-based solution of PANI is sufficiently stable for the electrostatic adsorption, which can adsorb onto both the substrates and anionic azo-polyelectrolyte surfaces. Through the layer-by-layer deposition scheme, thin films containing polycation/polyanion pairs with predetermined layer numbers can be obtained.

3.1. Multilayer formation

The multilayer growth process was studied by UV–vis spectroscopy and optical ellipsometry. Fig. 2 shows the UV–vis absorption spectra of the PANI/PNACN multilayer films with different numbers of bilayers. The pH of PANI and PNACN dipping solutions was 4.0 and 5.1, respectively. The multilayers exhibit three absorption bands at around 320, 450 and 630 nm. The strong absorption band at 320 nm can be attributed to the π–π^* transition centered on the benzene rings. The absorption band at 450 nm is due to the π–π^* electronic transition of the conjugated *trans*-azobenzenes and the band at 630 nm is due to the excitonic absorption of neutral PANI. It can be seen from the figure that the absorption intensity of the bands gradually increases as the number of bilayers increases. Fig. 3(a) shows the dependence of the absorbance at 630 nm on the number of bilayers. The layer-by-layer growth of the multilayer film is revealed by the linear increase in the absorbance with the increase of the number of bilayers. Fig. 3(b) gives the ellipsometric thickness of the multilayer as a function of the number of monolayers. The result further confirms the alternate growth of PANI and PNACN on a silica wafer. The average thickness of each PANI layer is about 2.48 nm and that of PNACN is about 0.58 nm. The thickness difference between PANI and PNACN layers can be attributed to the solubility difference of PANI and PNACN in the aqueous solutions. The PANI dipping solution was obtained by diluting organic solution of the undoped Emeralding-Base with the acidic medium, which produced partially doped PANI. Although the solution can show sufficient stability, the solvent is relatively "poor" to the PANI chains [8]. Therefore PANI chains have a tendency to transfer from the solution to the substrate. On the other hand, PNACN molecules are well dissolved in the solution and possess the stretched conformation because of the charge interaction.

The thickness of each layer can be altered by adjusting the pH of PANI and PNACN dipping solutions. Fig. 4(a) and (b) shows the influence of the pH of PANI dipping solutions. The multilayers were obtained by deposition in PANI solutions with the pH of 3.0, 3.5 or 4.0 and PNACN solution with the pH of 5.1. The absorbance at 630 nm and the thickness of the multilayer are given in the figures as a function of the number of bilayers. As the pH of the PANI solutions increases, the multilayer films show a larger thickness increase after each deposition cycle. The doping degree of the PANI is closely related to the solution pH. With the increase

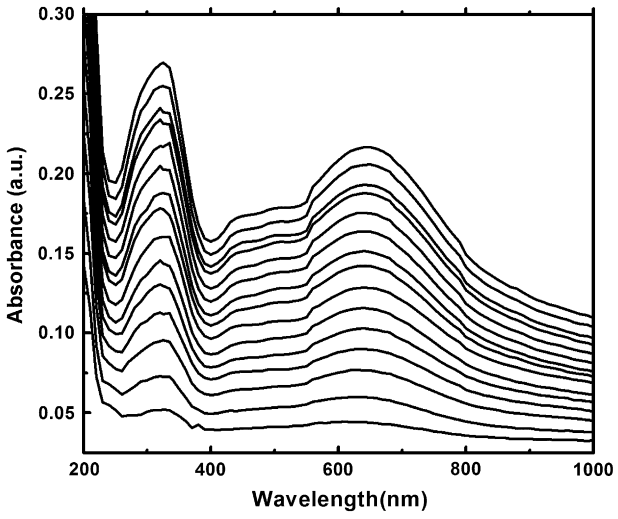

Fig. 2. UV–vis absorption spectra of PANI/PNACN multilayers with different numbers of the bilayers, 1–15 from bottom to top.

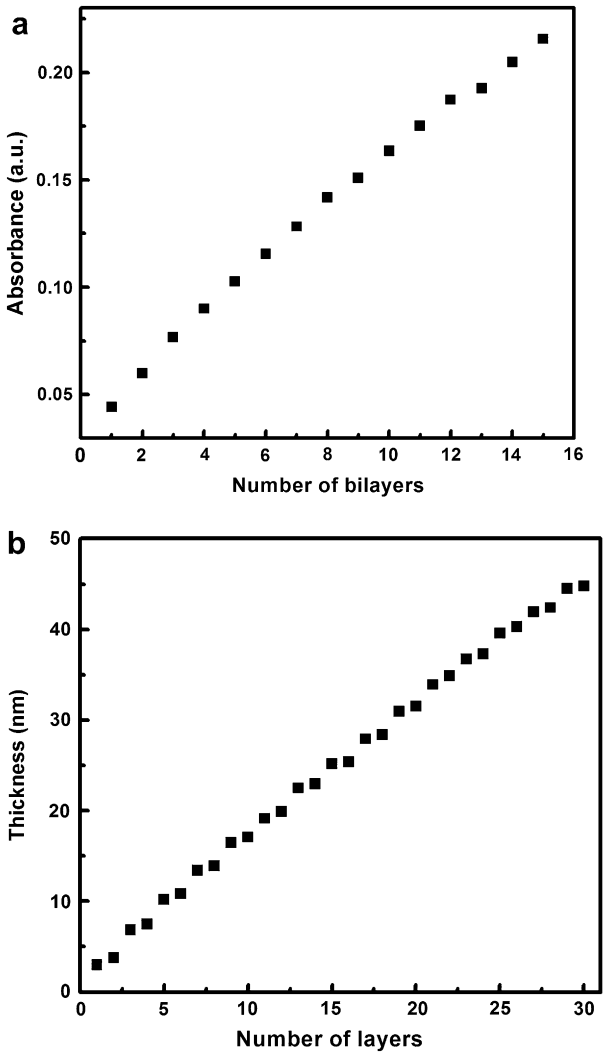

Fig. 3. (a) The absorbance at 630 nm of the multilayer films versus the number of bilayers, and (b) the total thickness of the films versus the number of layers.

of the pH, the doping degree and the charge density of the PANI chains decrease, which reduces the solubility of PANI in the aqueous solution. As a result, PANI chains are easier to be deposited on the surfaces with the pH increase. Fig. 4(c) and (d) shows the influence of the pH of PNACN dipping solutions. The multilayers were prepared by using a PANI dipping solution with pH of 4.0 and PNACN solutions with the pH of 5.1, 6.5, or 7.9. The plots show the dependence of the absorbance and thickness on the number of bilayers for the series of PNACN solutions. As pH of the PNACN solutions decreases, the thickness increase of each deposition cycle becomes larger for the multilayer films. The multilayer film obtained by using the PNACN solution with pH of 5.1 shows the largest absorbance and thickness increase with the increase of the bilayer number. This behavior is typical for the electrostatic adsorption of weak polyelectrolytes, which has been intensively investigated and reported [11].

The AFM and SEM observations show that the multilayer films possess a smooth surface with a mean roughness (Ra) of 6.9 nm. Fig. 5(a) and (b) gives typical AFM and SEM images of the surface morphology of a 15-bilayer PANI/PNACN film on a quartz slide. The multilayer was obtained by using the dipping solutions of PANI and PNACN with pH of 4.0 and 5.1, respectively. It has been reported that the surface roughness of the multilayer containing a weak polyelectrolyte can be reduced by adjusting the pH of its dipping solution [6]. However, for PANI/PNACN multilayers prepared by using the dipping solutions with different pH, a similar morphology and roughness were observed in the tested pH range. As the surface roughness related to the PNACN layers should be altered by adjusting the pH of the dipping solutions, the result seems to indicate that the surface roughness is predominantly controlled by the PANI layers. To maintain the stability of the dipping solutions, the pH of the PANI solutions can only be adjusted in the narrow range, which might not be enough to significantly influence the chain conformation and aggregation state of PANI in the solutions.

The formation and surface morphology of PANI/PPAPE, PANI/PNANT, and PANI/PNATZ multilayers are very similar to those presented above for the PANI/PNACN multilayers. Linear increases in the absorbance and film thickness can also be observed as the bilayer number increases. The pH variation of the azo-polyelectrolyte dipping solutions shows a similar effect as that of the PNACN solutions. A remarkable difference is that the maximum absorption bands of the azo polyelectrolytes appear at different wavelengths. This will influence the absorption spectra and electrochromic behavior of the multilayer films, which will be discussed in Section 3.4.

3.2. Cyclic voltammetry behavior

The redox behavior of the multilayer films was studied by cyclic voltammetry. In the electrochemical investigation, the PANI/PNACN multilayer films were deposited on the ITO glasses which were pretreated to be hydrophilic [23]. The PANI/PNACN multilayer films were immersed in a H_2SO_4 (0.1 M)/KCl (0.1 M) solution. As a control, the cyclic voltammograms (CVs) of PANI thin films were measured under the same condition with different scanning rates. The PANI monolayer thin films show typical CV curves for PANI in acidic solutions (the figure is not presented here). The oxidation peaks appear around 205 mV and 682 mV, while the corresponding reduction peaks are around 64 mV and 628 mV. The two oxidation peaks correspond to the transitions from the fully reduced insulating form (Leucoemeraldine) to the partially oxidized conducting form (Emeraldine Salt) and from the Emeraldine Salt to the fully oxidized insulating form (Pernigraniline) [48,49]. The two reduction peaks reveal the backward transitions with the hysteresis. Fig. 6(a) gives the CVs of a PANI/PNACN bilayer film at different scanning rates. In addition to the redox peaks observed for PANI monolayer films, a new pair of the redox peaks comes out at around 534 mV (the oxidation peak) and 519 mV (the reduction peak). These peaks have been identified as belonging to the water-soluble degradation products [24]. The peak currents linearly increase as a function of scanning rates. This result indicates that the surface control is dominant in the electrochemical processes of the PANI/PNACN bilayer films. The CVs of multilayers with the different numbers of bilayers were also investigated. The CV curves show a similar shape as those given for the bilayer films. The CVs of a PANI/PNACN films containing 15 bilayers are shown in Fig. 6(b) as a typical example. The peak potential shifts from 682 mV for the bilayer films to 740 mV for the multilayer. A similar increase (from 757 to 764 mV) has been observed for PANI/PSS multilayer films, which has been attributed to the increase in polaron/bipolaron states with the increment in bilayer number [23]. The peaks at around 534 mV become hardly perceived with the increase of the number of bilayers. The area of oxidation process in CVs at each scanning rate is equal to that of the reduction. There is a linear increase in the area of oxidation peaks as the number of the bilayers increases (Fig. 6(c)), which indicates that the redox capability is directly related to the amount of the electroactive material in the self-assembly films.

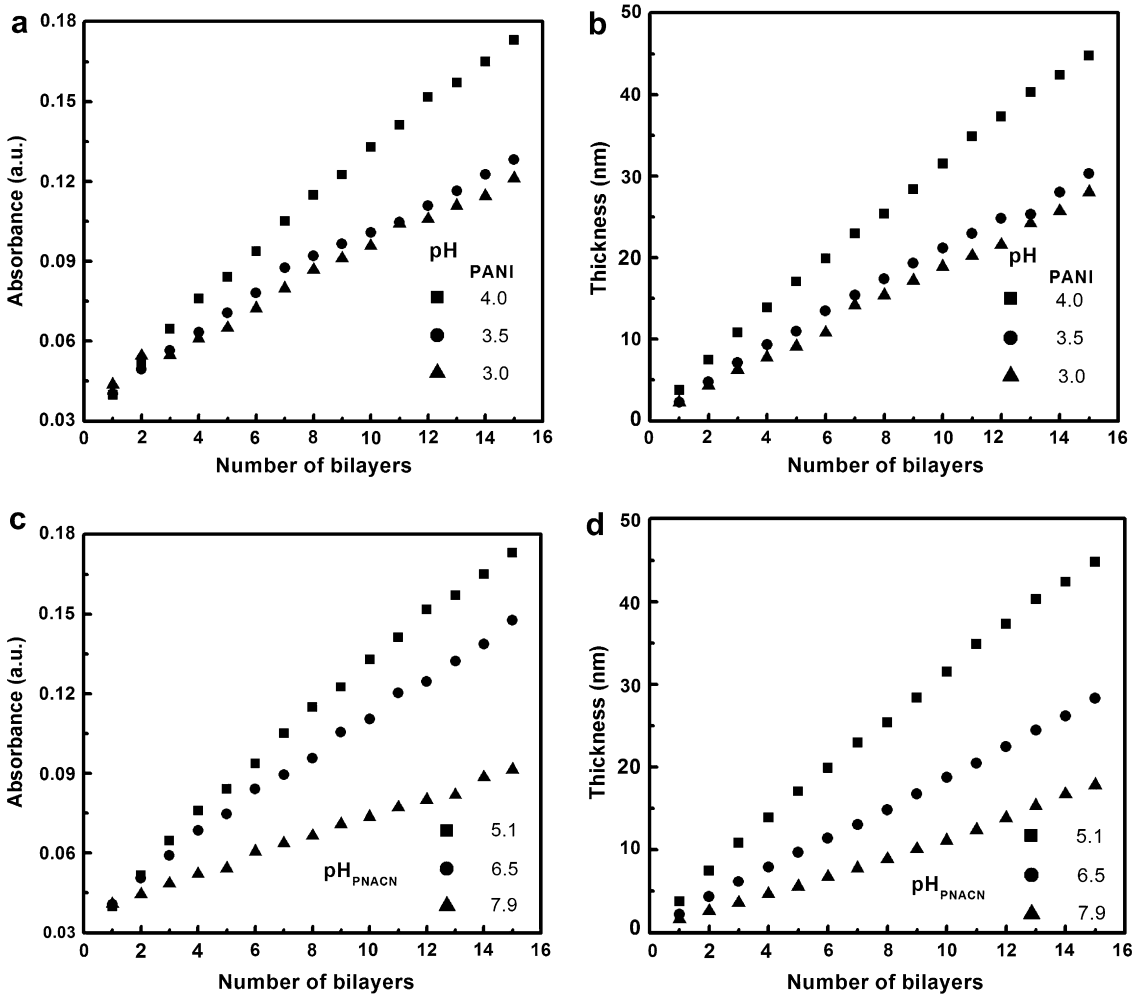

Fig. 4. The absorbance at 630 nm and thickness of the PANI/PNACN versus the number of bilayers. In (a) and (b), the pH of PANI solutions is 3.0, 3.5, 4.0 and the pH of the PNACN solution is 5.1. In (c) and (d), the pH of the PNACN solutions is 5.1, 6.5, 7.9 and the pH of the PANI solution is 4.0.

3.3. Photoresponsive properties

As a typical example of the multilayer films containing the pseudo-stilbene-type azo chromophores, the PANI//PNACN multilayers can show significant photoinduced dichroic effect upon the irradiation of linearly polarized Ar^+ laser beam. A unique feature of the multilayers is that the photoinduced dichroic window can be adjusted by changing the doping degree of the PANI layers. Fig. 7 shows the photoinduced dichroism of PANI/PNACN multilayers composed of 30 bilayers, which was obtained from the dipping solutions with pH of 4.0 and 5.1 for the PANI and PNACN solutions. For Fig. 7(a), (b) and (c), the self-assembled films were dunked in solutions with pH of 1, 4 and 9 for 60 min to adjust the doping degree of PANI and were carefully dried before the test. The UV–vis spectra of the multilayers were recorded before and after being irradiated with a linearly polarized Ar^+ laser beam (488 nm, 80 mW/cm^2) for 30 min. When the pH of the solution changes from 1 to 9, the absorption band of PANI shifts from 880 nm (polaron/bipolaron of doped PANI) to 630 nm (neutral PANI). As the band is partially overlapped with of the π–π^* transition band of PNACN, the spectral variation caused by the photoinduced dichroism is significantly altered in the three cases. The photoinduced dichroic variation caused by the linearly polarized light irradiation is due to the reorientation of the azobenzene moieties, which are driven to align perpendicularly to the direction of the electric-field vector of the incident light [27,29,30]. The orientation order parameter can be estimated from the polarized UV–vis spectra measured in the directions both parallel and perpendicular to the dominant orientation. The orientation order parameter can be obtained form the following equation [50],

$$S = \left(A_{\parallel} - A_{\perp}\right) \Big/ \left(A_{\parallel} + 2A_{\perp}\right)$$

where $A_{\parallel}$ and $A_{\perp}$ are the absorbance measured in the directions parallel and perpendicular to the dominant orientation direction. By this method, only the orientation order parameter of the highly doped multilayer can be obtained, where the π–π^* transition band of PNACN is not overlapped with the polaron/bipolaron absorption of PANI. The order parameter is estimated to be 0.031 for the PANI/PNACN multilayer doped with the acidic solution (pH = 1).

The photoinduced surface-relief-grating (SRG) formation of the PANI/PNACN multilayers was also studied. The 50-bilayer multilayer films were obtained from the dipping solutions with pH of 4.0 and 5.1 for the PANI and PNACN solutions, respectively. In the writing process, the multilayer films were exposed to the *p*-polarized interfering Ar^+ laser beams (488 nm, 100 mW/cm^2) at room temperature. The surface modulation was observed with AFM after 30 min irradiation. Fig. 8 shows a typical AFM image of the SRGs formed on the PANI/PNACN multilayer films. The spatial period of the SRGs is about 970 nm, which is coincident with the period of

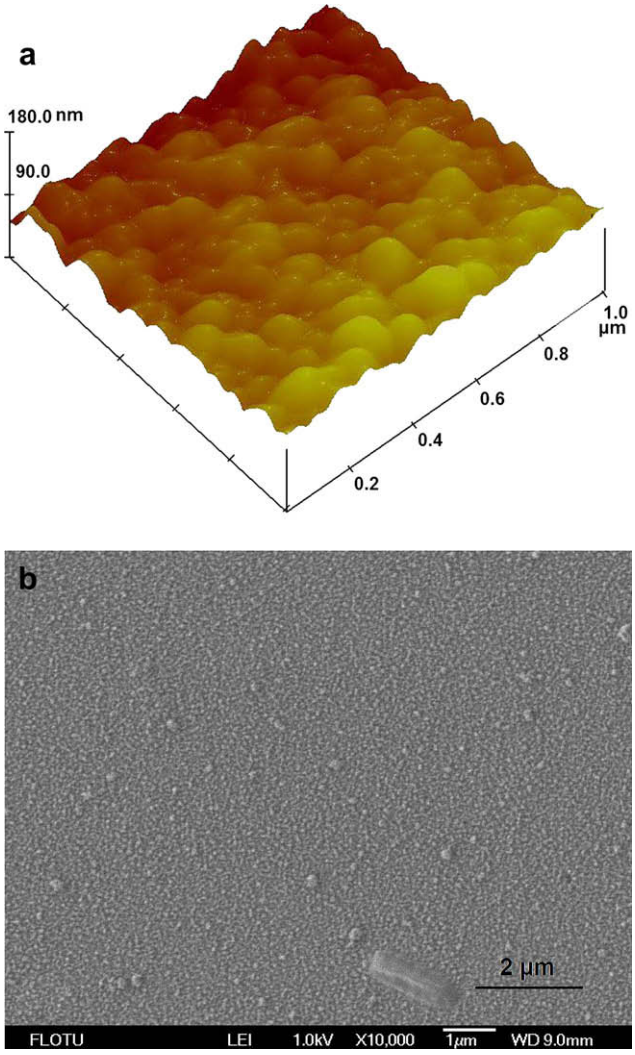

Fig. 5. The surface morphologies of the 15-bilayer PANI/PNACN film: (a) AFM, and (b) SEM images. The pH of PANI and PNACN dipping solutions is 4.0 and 5.1, respectively.

the interference pattern. The surface modulation height is about 32 nm, which is obviously smaller than the values reported for the spin-coated films [26]. The lower efficiency for the SRG formation has been observed for other electrostatic multilayers and attributed to the strong ionic bonds existing between polyanion and polycation layers [42]. For the current case, the PANI layers are much thicker than the PNACN layers. Therefore, the photo-driven PNACN layer motion could be severely restricted by the PANI layers.

3.4. Electrochromic properties

Because of the existence of the PANI component, the multilayer films can exhibit sensitive electrochromic variations. It is well known that azo chromophores can show various hues depending on their chemical structures [22,46]. By selecting polyelectrolytes bearing different azo chromophores, the color changes caused by the electrochromic PANI layers can be modified and enriched. The undoped PANI layers in the self-assembly films have two absorption bands at 320 nm and 630 nm. In the visible-light range (400–700 nm), there exists a transparent window in 400–500 nm, which results in the blue color of PANI. PPAPE has the absorption band at 335 nm, so the UV–vis spectrum of the PANI/PPAPE multilayer film is similar to that of the PANI film. On the other hand, PNACN, PNANT and PNATZ have the strong absorption at different wavelengths in

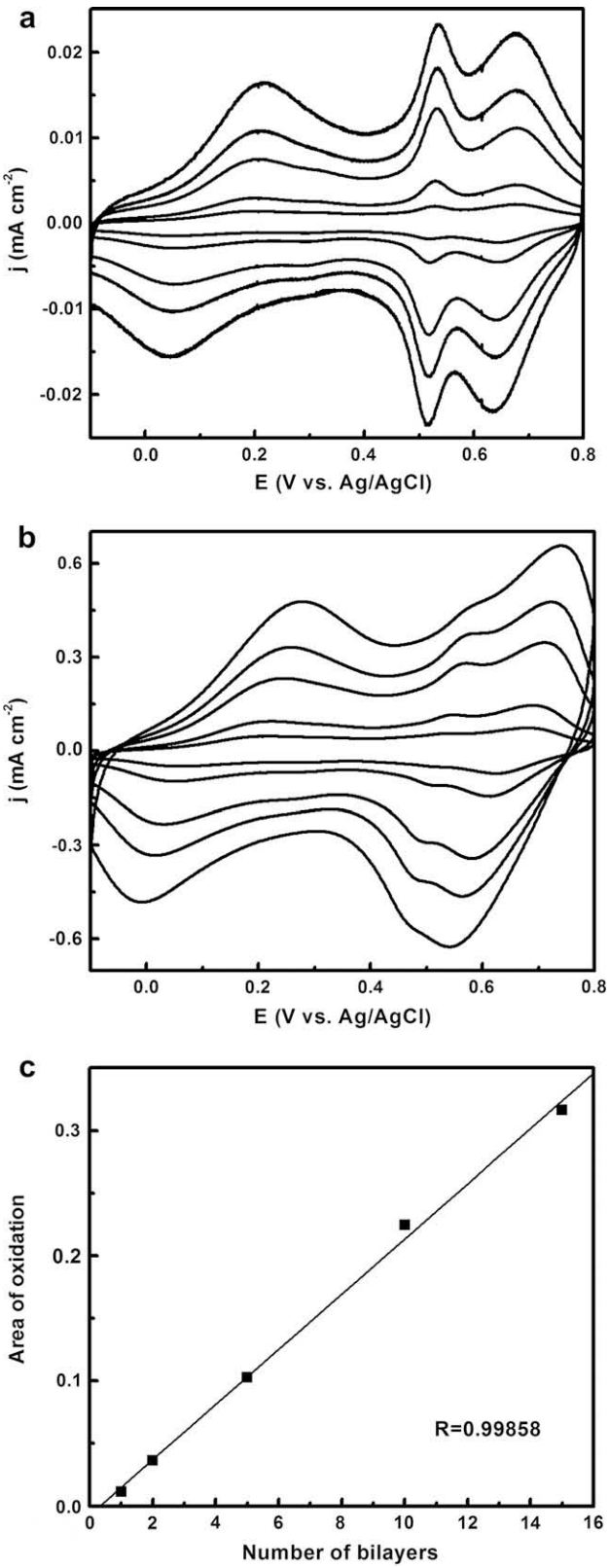

Fig. 6. (a) Cyclic voltammogram of a PANI/PNACN bilayer film at the scanning rates of 10, 20, 50, 70, and 100 mV/s. (b) Cyclic voltammogram of a 15-bilayer PANI/PNACN multilayer film at the scanning rates of 10, 20, 50, 70, and 100 mV/s. (c) Area of oxidation processes versus the number of bilayers at the scanning rate of 100 mV/s.

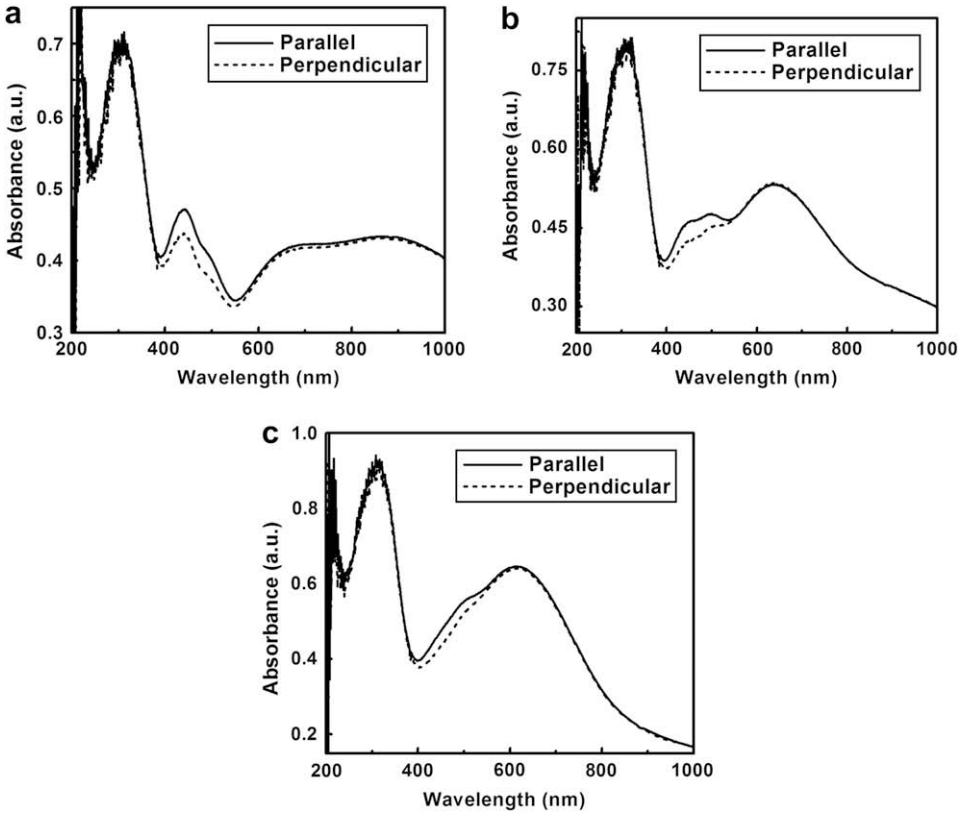

Fig. 7. Polarized UV–vis spectra of the 30-bilayer PANI/PNACN films, which were dunked in aqueous solutions with different pH and then dried: (a) pH = 1, (b) pH = 4, (c) pH = 9. Parallel and perpendicular mean the polarized UV–vis spectra measured at the parallel and perpendicular direction to the dominant orientation of azo moieties.

the visible-light range. The PNACN, PNANT and PNATZ layers can play important roles to influence the spectral characteristics and electrochemical color changes of the multilayers.

The 20-bilayer PANI/PNACN and PANI/PPAPE multilayer films are discussed here as two typical examples to illustrate the spectral features and electrochromic variations. The films were prepared by alternate deposition on ITO glasses through the electrostatic adsorption. The electrochemical investigations were carried out in a quartz cell filled with H_2SO_4 (0.1 M)/KCl (0.1 M) solution and equipped with two silver wires as the reference electrode and counter electrode. Fig. 9(a) shows the spectral response of the PANI/PNACN film in the different electrochemical redox states. The potentials are adjusted from −0.1 V to 0.8 V with a step size of 0.1 V. With the negative potentials, PANI layers are in the reduced Leucoemeraldine form. There is a weak absorption around 410 nm. As the oxidation proceeds with the potential increase from −0.1 to 0.8 V, the absorbance of 410 nm peak firstly increases and then shifts to 750 nm. In the 0.1 M H_2SO_4 solution, the oxidized PANI exists as the protonated Emeraldine salt (conducting form) with green color. After further oxidizations, the absorption around 410 nm is significantly depressed and PANI changes to the blue and insulating form. In the acidic environment, the PNACN is protonated and its π–π^* absorption band shows a red-shift from 452 nm to 500 nm. Therefore, the oxidized PANI/PNACN multilayer film shows strong absorption in the whole visible-light wavelength. Fig. 9(b) shows the electrochromic variation of PANI/PPAPE multilayer films with the change of potentials. Because the maximum absorption band of PPAPE appears at 335 nm, the oxidized multilayer films have a low absorbance in the range from 400 nm to 500 nm. The electrochromic variation of PANI/PPAPE multilayer films in visible-light range is similar to PANI.

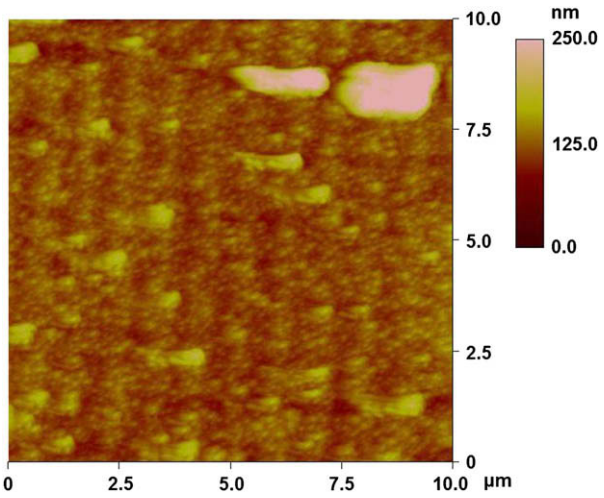

Fig. 8. A typical AFM image of the surface modulation of a 60-bilayer PANI/PNACN film after the Ar^+ laser irradiation for 30 min.

The electrochromic variations can be feasibly supplemented by using different azo polyelectrolytes and adjusting the relative thickness of the layers. The polyelectrolytes PNANT and PNATZ possess the maximum absorption bands at longer wavelengths, i.e. $\lambda_{max} = 518$ nm for PNANT and $\lambda_{max} = 548$ nm for PNATZ. The 30-bilayer PANI/PNANT and PANI/PNATZ multilayer films were constructed on the ITO glasses. To modifying the multilayer spectra, the PANI dipping solution was diluted to half the concentration used for Fig. 9(a) and (b). Fig. 9(c) and (d) shows the spectral variations of the PANI/PNANT and PANI/PNATZ films in the different

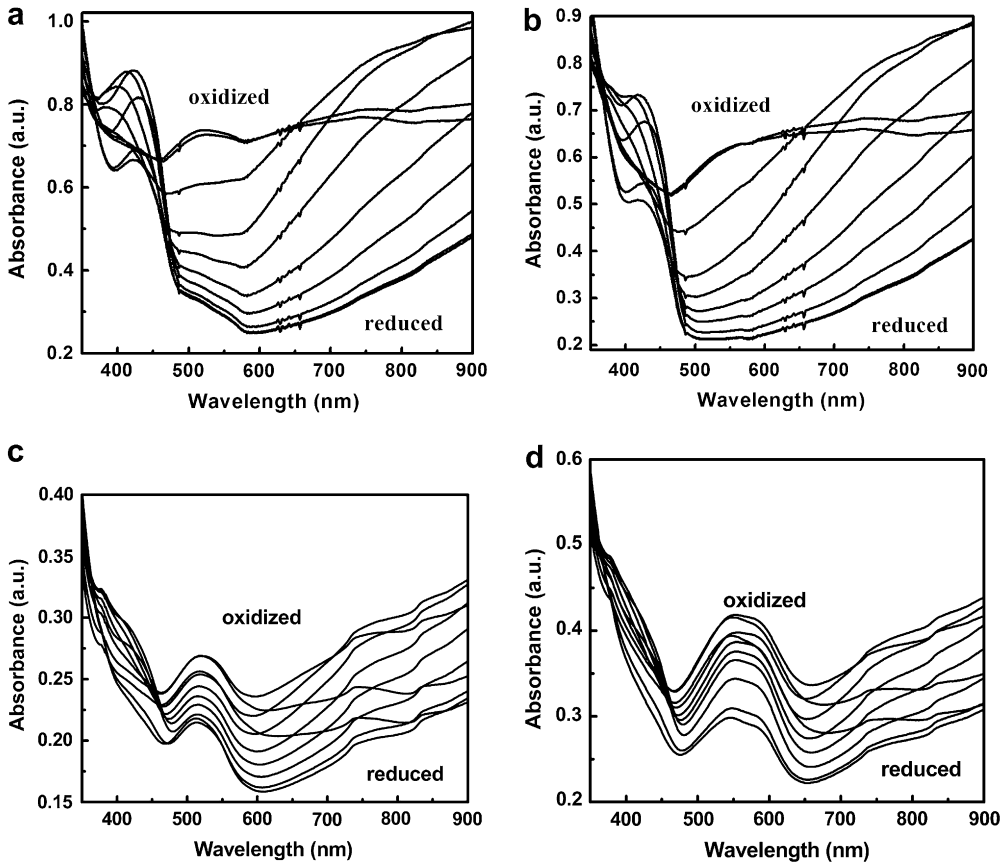

Fig. 9. UV–vis spectra of the multilayer films with different redox potentials, (a) 20-bilayer PANI/PNACN film, (b) 20-bilayer PANI/PPAPE film. (c) 30-bilayer PANI/PNANT film, (d) 30-bilayer PANI/PNATZ film. The potential was changed from −0.1 V to 0.8 V with step size of 0.1 V.

electrochemical redox states. The spectral variations of the PANI layers with the potentials are similar to those in PANI/PPAPE and PANI/PNACN films. However, because of the absorption of the PNANT and PNATZ layers, the spectral features and their variations are significantly modified for the PANI/PNANT and PANI/PNATZ multilayer films.

Fig. 10 gives the photographs of PANI/PNACN and PANI/PPAPE multilayer films under some typical potentials. The PANI/PNACN film shows the color switching from yellow-green (−0.1 V), to deep green (0.4 V) and then to black (0.8 V) (Fig. 10(a)). Under the same condition, the color of the PANI/PPAPE self-assembly films is changed from yellow-green (−0.1 V), to blue-green (0.4 V) and then blue (0.8 V) (Fig. 10(b)). The results show that the color change caused by the electrochromic variation of PANI can be significantly supplemented by using azo polyelectrolytes with different hues. For potential applications, the electrochromic windows can also be extended by adjusting the relative amount of the chromophores in the multilayer films, using azo polyelectrolytes with different DFs, or using other polyelectrolytes with opposite charges in some of the layer-pairs instead of the strict alternation of PANI and azo polyelectrolytes.

3.5. Electrical conductivity

As the PANI dipping solution with pH of 4.0 was used, the PANI/PNACN films were partly doped during the electrostatic self-assembly process and could show conductivity for the charge-carriers. To obtain multilayers with high and stable conductivity, the self-assembled films were immersed in the 1 M HCl solution for 30 min, and blown dry with the cold air stream. The in-plane electrical conductivities of the multilayer films were measured by the standard van der Pauw four-probe methods [51]. The conductivity of the 30-bilayer PANI/PNACN film can reach 0.02 S/cm. To find out the influence of the insulating layers in the self-assembly film, a 15-tetralayer PANI/PNACN/PDAC/PNACN film and a 10-hexalayer PANI/PNACN/PDAC/PNACN/PDAC/PNACN film were fabricated. The conductivities of these two films are 9.3×10^{-4} S/cm and 5×10^{-6} S/cm, respectively. With the increase of the number of PDAC/PNACN bilayers, the conducting polyelectrolyte (PANI) layers in the self-assembled films are gradually isolated with

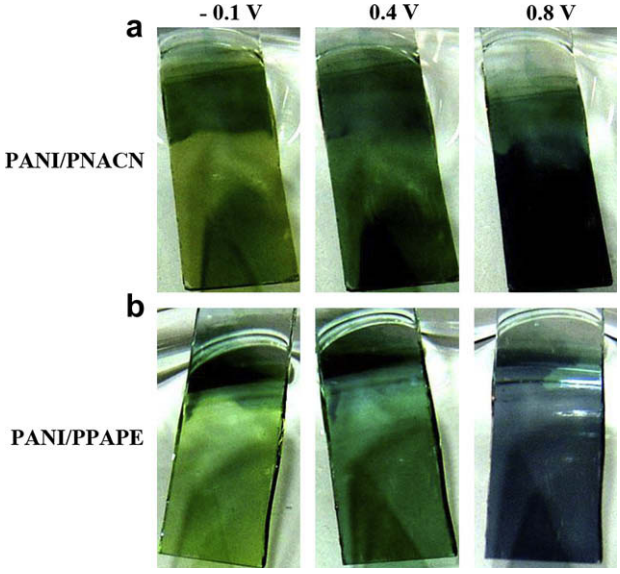

Fig. 10. Photographs of multilayer films at different oxidation states: (a) PANI/PNACN multilayer, (b) PANI/PPAPE multilayer.

each other. Moreover, the surfaces of the multilayer films are covered by the insulating layers which block the contact between the probes and the PANI layers. On the other hand, in PANI/PNACN multilayers, the PANI layers could be partially interpenetrated, which form the pathway for the charge-carriers.

4. Conclusions

The multilayer films of PANI and four-type azo polyelectrolytes have been successfully prepared through the electrostatic alternate deposition scheme. The multilayer thickness shows a linear increase with the increase of the dipping cycles. The single layer thickness can be adjusted by changing the pH of the PANI and azo-polyelectrolyte dipping solutions. The cyclic voltammetry investigation reveals that the multilayer films possess redox properties related to the PANI layers. The PANI/PNACN multilayer shows photoinduced dichroism caused by the photoisomerization and subsequent reorientation of the azo chromophores, but its ability to form surface-relief-gratings is weak. As containing the electroactive PANI and colorful azo polyelectrolytes, the multilayer films can show sensitive and enriched electrochromic variations. By adjusting the hues of azo polyelectrolytes and the relative amount of both components in the multilayers, thin films with prosperous electrochromic variations has been demonstrated. After being doped with 1 M HCl solution, the PANI/PNACN multilayer film shows the conductivity of 0.02 S/cm.

Acknowledgements

The financial support from NSFC under Projects 50533040 is gratefully acknowledged.

Appendix. Supplementary data

Supplementary data associated with this article can be found in the online version, at doi:10.1016/j.polymer.2008.09.063.

References

[1] Decher G. Science 1997;277(5330):1232–7.
[2] Decher G, Hong JD, Schmitt J. Thin Solid Films 1992;210/211:831–5.
[3] Hammond PT. Curr Opin Colloid Interface Sci 1999;4(6):430–42.
[4] Schnhoff M. Curr Opin Colloid Interface Sci 2003;8(1):86–95.
[5] Hammond PT. Adv Mater 2004;16(15):1271–93.
[6] Ferreira M, Rubner MF. Macromolecules 1995;28(21):7107–14.
[7] Fou AC, Rubner MF. Macromolecules 1995;28(21):7115–20.
[8] Cheung JH, Stockton WB, Rubner MF. Macromolecules 1997;30(9):2712–6.
[9] Stockton WB, Rubner MF. Macromolecules 1997;30(9):2717–25.
[10] Dubas ST, Schlenoff JB. Macromolecules 1999;32(24):8153–60.
[11] Shiratori SS, Rubner MF. Macromolecules 2000;33(11):4213–9.
[12] Laurent D, Schlenoff JB. Langmuir 1997;13(6):1552–7.
[13] Watanabe S, Regen SL. J Am Chem Soc 1994;116(19):8855–6.
[14] Lvov Y, Ariga K, Ichinose I, Kunitake T. J Am Chem Soc 1995;117(22):6117–23.
[15] Lvov Y, Decher G, Sukhorukov G. Macromolecules 1993;26(20):6117–23.
[16] Lvov Y, Haas H, Decher G, Mohwald H, Mikhailov A, Mtchedlishvily B, et al. Langmuir 1994;10(11):4232–6.
[17] Su YZ, Dong W, Zhang JH, Song JH, Zhang YH, Gong KC. Polymer 2007;48(1):165–73.
[18] Peng H, Zhang LJ, Spires J, Soeller C, Travas-Sejdic J. Polymer 2007;48(12):3413–9.
[19] Huh DH, Chae M, Bae WJ, Jo WH, Lee TW. Polymer 2007;48(25):7236–40.
[20] Aydemir K, Tarkuc S, Durmus A, Gunbas GE, Toppare L. Polymer 2008;49(8):2029–32.
[21] Pytel RZ, Thomas EL, Hunter LW. Polymer 2008;49(8):2008–13.
[22] Ak M, Gacal B, Kiskan B, Yagci Y, Toppare L. Polymer 2008;49(9):2202–10.
[23] Ram MK, Salerno M, Adami M, Faraci P, Nicolini C. Langmuir 1999;15(4):1252–9.
[24] Park MK, Onishi K, Locklin J, Caruso F, Advincula RC. Langmuir 2003;19(20):8550–4.
[25] DeLongchamp DM, Hammond PT. Chem Mater 2004;16(23):4799–805.
[26] Delaire JA, Nakatani K. Chem Rev 2000;100(5):1817–45.
[27] Natansohn A, Rochon P. Chem Rev 2002;102(11):4139–75.
[28] Kumar GS, Nechers DC. Chem Rev 1989;89(8):1915–25.
[29] Eich M, Wendroff JH, Beck B, Ringsdorf H. Makromol Chem Rapid Commun 1987;8:59–63.
[30] Todorov T, Nicolova L, Tomova N. Appl Opt 1984;23(23):4309–12.
[31] Ichimura K, Suzuki Y, Seki T, Hosoki A, Aoki K. Langmuir 1988;4(5):1214–6.
[32] Ikeda T, Tsutsumi O. Science 1995;268(5219):1873–5.
[33] Rochon P, Batalla E, Natansohn A. Appl Phys Lett 1995;66(2):136–8.
[34] Kim DY, Tripathy SK, Li L, Kumar J. Appl Phys Lett 1995;66(10):1166–8.
[35] Lvov Y, Yamada S, Kunitake T. Thin Solid Films 1997;300(1–2):107–12.
[36] Wang XG, Balasubramanian S, Li L, Jiang XL, Sandman DJ, Rubner MF, et al. Macromol Rapid Commun 1997;18(6):451–9.
[37] Laschewsky A, Wischerhoff E, Kauranen M, Persoons A. Macromolecules 1997;30(26):8304–9.
[38] Toutianoush A, Tieke B. Macromol Rapid Commun 1998;19(11):591–5.
[39] Dante S, Advincula R, Frank CW, Stroeve P. Langmuir 1999;15(1):193–201.
[40] Wu L, Tuo X, Cheng H, Chen Z, Wang XG. Macromolecules 2001;34(23):8005–13.
[41] Hong JD, Jung BD, Kim CH, Kim K. Macromolecules 2000;33(21):7905–11.
[42] Wang HP, He YN, Tuo XL, Wang XG. Macromolecules 2004;37(1):135–46.
[43] Alva KS, Lee TS, Kumar J, Tripathy SK. Chem Mater 1998;10(5):1270–5.
[44] Huang K, Wan MX. Chem Mater 2002;14(8):3486–92.
[45] Rau H. In: Rabek JF, editor. Photochemistry and Photophysics, vol. II. Boca Raton, FL: CRC Press; 1990 [chapter 4].
[46] Mattoso LHC, Macdiarmid AG, Epstein AJ. Synth Met 1994;68(1):1–11.
[47] Wang XG, Yang K, Kumar J, Tripathy SK. Macromolecules 1998;31(13):4126–34.
[48] Wei Y, Focke WW, Wnek GE, Ray A, MacDiarmid AG. J Phys Chem 1989;93(1):495–9.
[49] Maia DJ, das Neves S, Alves OL, De Paoli M-A. Electrochim Acta 1999;44(12):1945–52.
[50] Andele K, Birenheide R, Eich M, Wendroff JH. Makromol Chem Rapid Commun 1989;10:477–83.
[51] van der Pauw LJ. Philips Tech Rev 1958/59;20(8):220–4.